AUTOMATIC ASSESSMENT FOR THE DETECTION OF KNEE EFFUSION USING MAGNETIC RESOURCE IMAGING

Aamir Yousuf Bhat, Research scholar*[1], A.Suhasini, Professor*[2],
Department of Computer and Information Science*[1]
Department of Computer Science and Engineering *[2]
Annamalai University

Abstract

Effusion of the knee joint is possibly related to osteoarthritis erupt and is a significant marker of remedial reaction. The investigation is planned for creating and approving a computerized framework dependent on MR imaging for the measurement of joint effusion. The occurrence of knee effusion requires an extensive differential determination and an orderly symptomatic approach. Yearning of the knee effusion is a fundamentally demonstrative and restorative intercession in numerous rheumatologic diseases. The clinical investigation has traditionally included tests counting the patella tap. The precision of these tests for identifying the effusion and measure is not well set up. MR imaging is considered superior for recognizable proof and evaluation of knee effusion. The amount of effusion present in the joint was recorded and MRI criteria for the detection of knee effusion were assessed. The fat cushion division sign was the foremost exact marker of liquid as little as 1-2 ml was recognized. Axial view of MRI images was used in accessing the knee effusion. The classifier was superior both in terms of time efficiency and classification performance to classifier regularly used on the basis of iterative learning. In this paper we have used two features namely watershed Segmentation and 2-D Gabor Filter. The extracted features from MRI image are given to the classifiers namely Random Forest, Multi Linear BPNN and Adaboost SVM. The random forest classifier was good when comparing with the other two classifier and achieves the good accuracy rate of 92.12 %. Finally the classifier was prevalent both in time adequacy and order execution to the routinely used classifiers dependent on iterative learning.

Index Terms: Knee Effusion, 2-D Gabor Filter, Random Forest, Multi-layer BPNN, Adaboost SVM, Osteoarthritis (OA).

1 Introduction

A joint effusion is an abnormal fluid accumulation in or around the knee joint. It is usually caused by infection, injury and arthritis. Knee is the most affected joint by effusion, although it can occur in ankle, shoulder and hip. There is more evidence that there is synovial inflammation. It plays an important role in OA pathogenesis of the knee. Synovial inflammation could be displayed as synovial membrane. MRI is the most common visualization method used to evaluate the presence and intensity of synovial inflammation. Thickening of the synovial membrane and joint effusion as determined by MRI are often measured together as a whole with the term effusion synovitis as a replaced for synovial inflammation. Joint effusion is often associated with joint disorders. In OA, effusion is an important factor epidemic markers and quantification. This can be useful as a measure of treatment results. The most common method used to measure joint effusion. The main weakness of this method; however besides being invasive and something that is painful, that you cannot often predict [1]. There is a certain sum of synovial fluid interior of any joint especially in expansive joint such as knee joint. The occurrence of normal amount of synovial fluid cannot be identified by clinical examination as well as by Ultrasound, but can be recognized by MRI [2]. For the development of the knee joint synovial liquid is secreted by type B cells of synovial membrane. Synovial fluid moves into the cartilage when a joint is on resting and moves out of the joint space, when the joint is dynamic especially weight bearing. Synovial fluid incorporates hyaluronic corrosive (HA) lubricin (PRG4), surface-active Phospholipids (SAPL) proteinase and collagenases [3]. Type A is phagocytic cells, which evacuates the wear and tear debris from the synovial fluid. HA and PRG4 increment the consistency and flexibility of articular cartilages and grease up the surface between synovium and cartilage.

The characteristics history of MRI detected effusion synovitis in older subjects has not yet been described. It is not known if the knee has structural abnormalities including cartilage defects, reduced cartilage volume, meniscal lesions and bone marrow lesions to produce effusion synovitis. Joint effusion can be distinguished visually from synovitis utilizing contrast enhanced MRI after intravenous gadolinium infusion, but method is most commonly utilized for investigation, since of potential side effects and high costs. Knee effusion can be classified as traumatic and non-traumatic. Non-traumatic etiologies incorporate degenerative joint pain, inflammatory arthritis, contamination, precious stone testimony and tumour [4]. There is obvious reason for knee effusion in case of fiery, irresistible, crystal deposition inflection and tumour case. The fore most common reason for degenerative joint pain is overuse repetitive push and dynamic life style. The exact cause of primary OA is still questionable. There is a decrease in the concentration of HA and SAPL in synovial fluid from primary OA patients by the obscure component [5].

During the recent years imperative advances has been made for the improvement of MRI innovation. Strategies have been created to assess quantitatively or semi-quantitatively the structural change that happens within the joint tissues incorporating the cartilage, synovial layer, menisci, subchondral bone during OA [6].The knee effusion may be common findings in patients with knee problems although patients may or may note that his knee is swollen. The clinical tests for identification of knee effusion routinely utilized at present time are patella tap test, fluid test and fluctuation test. The occurrence of knee effusion can be affirmed by MRI, USG, circumferential estimation utilizing a measure tape comparing the estimate of the both knees and volumetry utilizing water uprooting as a cruel to identify limb volume [7]. For the identification of large amount of effusion patella tap and cross change tests are used and for the identification of small amount of effusion, fluid shift tests are utilized.

2 Materials & Methods

Dataset

The dataset used for the experiment are obtained from various clinical centres and hospitals. The dataset compromises the information of 250 patients with 40 to 60 years of ages, which has MRI measurement at base line and follows up. MRI was taken on 1.5-T whole body scanner. The MRI examination compromised of two sequences in axial planes without patient repositioning. T2 weighted gradient echo true fast imaging with steady state precision sequence (T2 true FISP, TR/TE I 6/3 ms, ST/SS, 3/0 mm; FOV, 160mm, FA, 90 degrees; NEX, 2; matrix, 320×320 pixel; reconstructed image, 320×320 pixel; voxel size, 0.5×0.5×3mm^3) and T1 weighted in phase, out phase gradient echo (GRF) sequence (in TR/TF, 450/2.6ms; out-TR/TF, 450 ms; 6.4 ms; ST/SS, 3/0 mm, FOV, 180×144mm; FA, 70 degrees; NEX, 1; matrix 320×256pixel; reconstructed image, 640×512 pixel and voxel size 0.28×0.28×3mm^3).

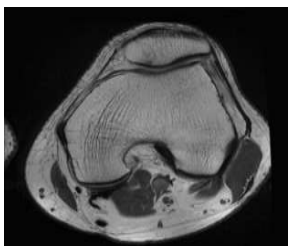

Figure 1(a) Axial view of Normal knee joint

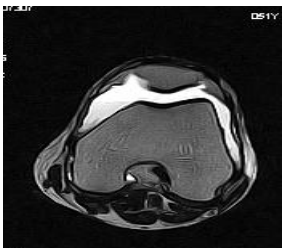

Figure 1 (b) Effusion in Knee Joint

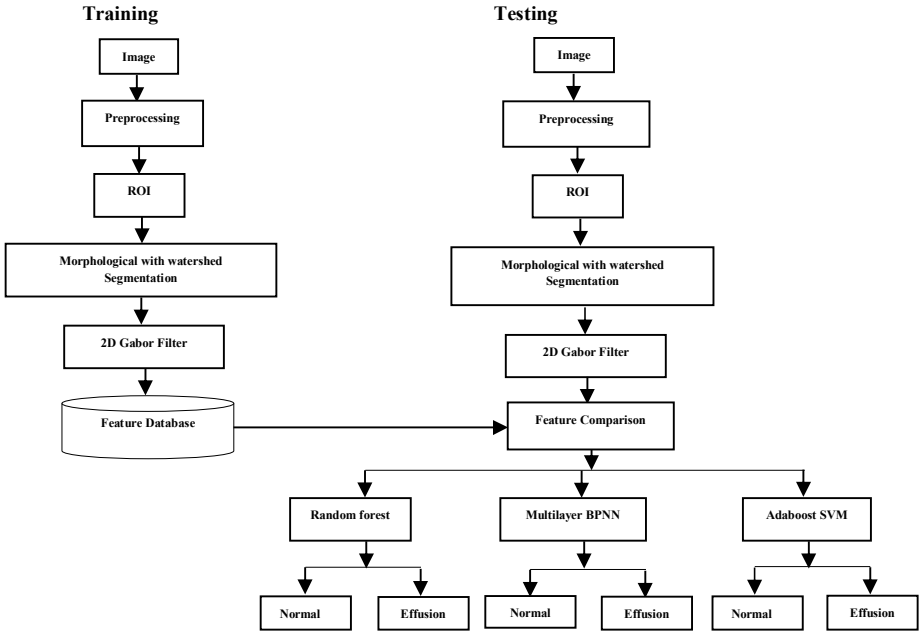

Figure 2 Block Diagram for proposed Methodology for Knee Effusion

Preprocessing

The pre-processing of pictures commonly includes evacuating low frequency background noise, normalizing the intensity of the indidual particles pictures, expelling or improving information pictures earlier to computational processing. The goal of pre-processing is an improvement in the picture information that smoother undesirable mutilations or improves a few picture features for further processing. Four classifications of picture pre-processing strategies concurring to the measure of the pixel neighborhood that is utilized for the calculations of unused pixel brightness, pixel brightness transformation, pre-processing techniques that utilize a local neighborhood of the processed pixel, geometric transformation, image restoration that requires knowledge about the entire image.

We have used weiner filter to remove the background noise from the MRI image. Weiner filter is not an adaptive filter, because it expects input to be stationery. It takes a measurable approach to take its goal. Goal of the filter is to expel the noise from a signal. Before usage of the filter, it is expected that the user knows the spectral properties of the initial signal and noise. Spectral properties are just like the control functions for both the initial signal and noise. The resultant signal requires is as near to the original signal. Signal and noise are both stochastic procedures with known spectral properties. The point of the method is to have minimum mean square error. That is the distinction between the first signal and the new signal should be as less as could reasonably expected. The weiner filter is ideal in terms of the mean square error. In other words it minimizes the general mean square error within the process of inverse filtering and noise smoothening. The weiner filter may be a direct estimation of the original picture. The methodology depends on the stochastic system. The symmetry rule infers that the weiner filter in Fourier space can be defined as:

$$G(u,v) = F(u,v).H(u,v) \quad (1)$$

F is the Fourier transform of original picture. H is the blurring function. H (u, v) is the received signal and G (u, v) is the restored image.

Image Segmentation

Image segmentation is a basic procedure for most consequent picture investigation assignments. In specific numerous of the existing strategies for picture portrayal and acknowledgement, picture visualization and object based picture compression profoundly depend on the division results. The common division includes the apportioning of a given picture into a number of homogenous sections, such that the union of any two neighboring sections yields a heterogeneous section. On the other hand division can be considered as a pixel naming procedure, as in all pixels that have a place with the equivalent homogenous area is appointed a similar mark. There are a few different ways to characterize homogeneity of a region based on the specific objective of the division procedure.

3 Feature Extraction

3.1 Watershed Segmentation

The present techniques for picture fundamentally utilize two thoughts. One of them is finding the form of objects in the picture. The other is gathering focuses with similar characteristics, so that the object of interest is completely recreated. The issue of contour distinguishing proof may be illuminated with the utilization of the watershed administrator, which is the primarily morphological segmentation division tool known as water line. An instinctive thought of the watershed idea might be formed considering the gray levels picture as a topographic surface and expecting that gapes have been punctured in each territorial least of the surface. The surface is then gradually emerged into water. Beginning from the base at the most minimal height, the water will progressively flood the maintenance basins of the picture. In expansion, dams are raised at the places, where the water coming from the unique essentials would rise. Towards the part of this flooding strategy, each least is encompassed by dams portraying its associated retention basin. The entire arrangement of dams compare to the watersheds. They provide us with portion of an input picture into its distinctive basins [16]. Watershed related to the regional minimums set $M = U_i \in_R mi$of an image S may be characterized as the union complement of all maintenance basins $C_f(m_i)$ and can be defined by the following equation as:

$$WL(f) = [\, U_i \in_R C_f(m_i)]^c \qquad (2)$$

Watershed segmentation is a powerful scientific morphological tool for the picture division. It is most used in medical image processing and computer vision [20]. Watershed implies the edge that partitions ranges drained by distinctive waterway frameworks. In the event that picture is seen as topographical scene, the watershed lines decide limits which isolate picture regions. The watershed change registers catchments basins and ridge lines, where catchments basins comparing picture areas and ridge lines identifying with area limits. Watershed segmentation dependent on watershed change have fundamentally two classes [21]. The first class contains the flooding based watershed segmentation, whereas the second class contains rain falling watershed algorithms. Numerous algorithms have been proposed in the two classes, but associated components based watershed algorithm appears exceptionally great execution compared to all others. It comes under the rain falling based watershed algorithm procedure. It gives exceptionally great division results and meets the criteria of less computationally complexity for hardware execution.

Watershed Transform

It is an effective mathematical morphological tool for the picture division. Watershed algorithm involves three essential steps (1) gradient of the image (2) flooding (3) segmentation. In the initial

step, the slope of the picture is calculated [17]. It demonstrates the directional change in the color of the picture. The next step includes the development of the catchment basin and flooding [18]. In this step, on the off chance we consider the picture a scene picture at that point the gap is punctured there, where the power is exceptionally low. Moreover where the gap is punched, that is called as the catchment basin. After that the flooding procedure begins, when that topographic relief is overwhelmed with water, the separate lines of the areas falling over the locales structure of the watersheds. Naturally a drop of water falling on a topographic relief steers towards the closest minimum. The closest minimum is that minimum which lies toward the part of the steepest plunge. These minima are the neighborhood minima. The water topped of at the beginning nearby minima and focuses, where water coming from various basins would meet and dams will be worked. The third step prompts the development of dams [19]. In light of the fact that towards the part of the arrangement procedure dams come into record and these dams shapes the unbending watershed lines. These dams maintain a strategic distance from an occasion, which comes during the flooding, when at least two floods coming from various minima may consolidate. These dams characterize the watershed of the capacity of a picture. This isolates the various catchments basins.

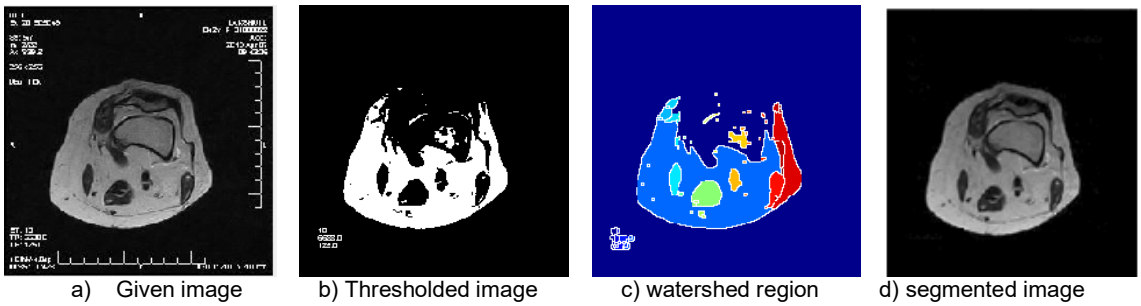

a) Given image b) Thresholded image c) watershed region extraction d) segmented image using watershed segmentation

Figure 3 Watershed Segmentation of knee joint in axial view

3.2 2-D Gabor Filter

Gabor filter is a linear filter utilized for the detection of an edge. The frequency and direction portrayals of Gabor filters are like those of human visual framework and they have been observed to be especially fitting for surface portrayal and separation. In the spatial domain a 2D Gabor filter is a Gaussian kernel function adjusted by a sinusoidal plane wave. The Gabor filters are self-comparative; all filters can be created from one mother wavelet by dilation and rotation. The 2D complex Gabor filter is particularly useful for removing a set of characteristics in multiple orientations and frequencies of an image [8]. Complex 2D Gabor filtering for all pixels for an image however; causes an expanse costs. With the Gabor core defined in a specific orientation and frequency, filtering is done by moving a reference pixel by pixel. The core complex of Gabor hinders fast filtering in context similar to filters with edge recognition [9].

To speed up 2-D complex Gabor filter, a few efforts have been made for occurrence by making utilize of FFT (Fast Fourier Transform), IIR (Infinite Impulsive Response) filters of finite impulsive response (FIR) filters. It was appeared [10] that Gabor filter for 1-D signal of N tests can be performed with the same complexity as of the FFT O ($N\log_N$). In [11] distinct FIR filters are connected to perform quick 2D complex Gabor filtering by exploiting special relationship between the Gabor parameter in a multi-resolution pyramids.Its impulsive reaction is characterized by a harmonic function motivated by a Gaussian function. In light of the multiplication convolution property, the Fourier change of a Gabor filters motivation reaction is the convolution of the Fourier change of the

harmonic function and the Fourier change of the Gaussian function.The filter contains a genuine and an imaginary component speaking to orthogonal headings. The two components may be shaped into a complex number or utilized separately. A 2D Gabor filter is defined as:

$$\left\{\frac{1}{2\pi}\sigma x\ \sigma y \exp\frac{1}{2}\ x\right\}\ g(x,y) = \frac{1}{2\pi}\ \left\{\boldsymbol{\sigma x\ \sigma y}\quad \boldsymbol{exp}\frac{\mathbf{1}}{\mathbf{2}}\quad (\boldsymbol{x^2/\sigma^2_x}\right\}+\boldsymbol{y^2/\sigma^2_y}) \qquad (3)$$

The spread of the Gaussian work in x and y directions have been signified by σx and σy symbols separately. The Gabor channel bank is connected on the pictures considering the focus recurrence to mean the direction of the filters. In the recurrence area the Gabor filter depends on the two dimensional 2D recurrence and direction. In this paper we take over eight diverse direction and recurrence situations and a Gabor space is made by convolving these channels with the test pictures. The recurrence response of the filter is given by the equation.

$$H(u,v) = 2\pi\ \ \sigma_x\,\sigma_y[\exp(-2\pi^2[a+b)] \qquad (4)$$

Where $a = [(u-u_0)^2\ \sigma^2 x]$ &b=$[(v\text{-}v_0)^2\ \ \sigma^2 y]$. In this way Gabor function can be thought as being a Gaussian work moved in recurrence.

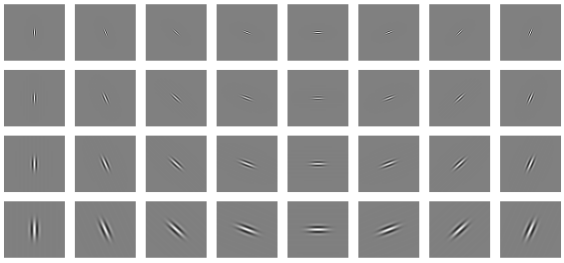

Figure 4 2-D Complex Gabor Filter with 32 coefficients (4 Frequencies and 8 orientations)

The middle recurrence of the filter is indicated by the recurrence of the sine/cosine wave and the bandwidth of the channel is balanced by the width of the Gaussian. A 2D Gabor filter over on image space (x, y) as:

$$G(x,y) = \theta^{-\pi}[(x-x_0)^2]/\alpha^2+[(y-y_0)^2)/\beta^2]\sigma^{-2\pi t}[u_0(x-x_0)cos\theta] + [v_0(y-y_0)]sin\vartheta] \qquad (5)$$

X_0 and y_0 represents positions in the image, (α, β)represents the effective width and length and (u_0, v_0) represents specific modulation which has spatial frequency.

4 CLASSIFICATION

4.1 Random Forest

Random forest is a machine learning that is progressively being utilized for classification and regression consists of an ensemble of independent decision tress. It is a group of model which implies that it utilizes the outcomes from a wide range of models to ascertain a reaction. In most cases the result from an ensemble model will be superior to the result from ant one of the personal model. Within the case of Random forest a few choice tress are made and the response is calculated based on the result of all the choice tress. It consists of a number of trees, where each tree is developed employing a shape of arrangement. The leaf nodes of each tree are labelled by gauges of the ensuing dispersion among the sorts of pictures. Each node inside the tree follows a test that separates the space superior of information to classify. An image can be classified by sending it down through each tree

and accumulating to come to leaf distributions. Randomness can be infused at two cases amid in training: In sub-sampling of training information, so that each tree is developed employing a distinctive subset and when selecting the nose testing.

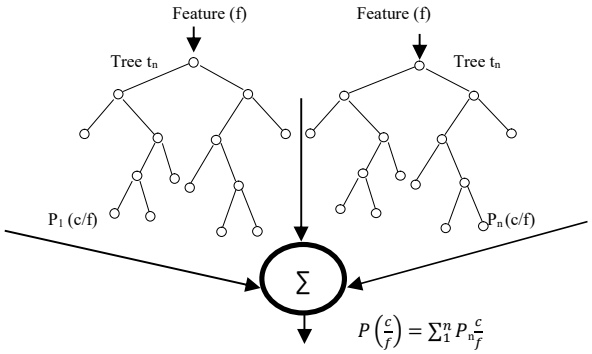

Figure 5 Random Forest

The trees are binary and built from in a top-down way. Binary tests at every node can be picked in one of the two different ways (1) randomly (2) by combining the yield of different randomized trees into a single classifier. They have been illustrated to deliver lower test errors than conventional decision trees [12].The best here is measured by the data gain caused by dividing the set of Q illustrations into two subsets Q_i, concurring the given test.

$$\Delta E = -\sum i \frac{|Qi|}{|Q|} E(Qi) \qquad (6)$$

E(q) is the entropy $-\sum_{j=1}^{n} p_j \, log2 \, (pj)$with pj the extent of illustrations in q having a place with class j, and $|.|$ the size of the set. The procedure of choosing a test is repeated for each non-terminal node utilizing as it were the preparing illustrations falling in that node. The recursion is halted when the node gets excessively few models. If we assume that T is the size of all trees, C is the set of all classes and L is the set of all clears out for a given tree. Amid the preparing stage the back probabilities $(P_{t,\,l}(Y(I) = c)$for each class c ∈ Cat each leaf node l ∈ L are found for each tree t ∈ T. These probabilities are determined as the proportion of the quantity of pictures I of class c that arrive at l to the absolute number of pictures that arrive at l. Y (I) is the class name c for picture I.

Classification- The image for testing purpose is passed down each random tree until it comes to a leaf node. All the back probabilities are at that point found the middle value of the arg max is taken as the classification for the input picture. It is a decision tree gathering classifier with each tree developed utilizing a few sort of randomization. Random forests have a capacity for preparing huge amount of information with high preparing spaces in view of a choice tree. The structure of each tree in the random forest is twofold and is made in a top-down way as shown in figure 5. In this work we consider binary trees with their structure and choice nodes learned discriminatively as pursues. Beginning from the root given the named preparing data, the function t and thresholdλ, which maximize the data pick up are found. Then preparing continues down to the children nodes.

In the preparing technique the random forest begins by picking an arbitrary subset I from the neighborhood of Gabor filter preparing information. At the node n the preparing information $I_n$is iteratively split into left and right subsets I_l and I_r by utilizing the limit t and split function F (v_i) for the feature vector v using equation 5. The threshold t is arbitrarily picked by the split function F (v_i) in the range $t \, \epsilon \, (\min F(v_i) \max F(v_i))$

$$Il = \{ i \epsilon I_n / f(v_i) < t \} \quad (7)$$

$$I_r = I_n / I_l \quad (8)$$

At that point a few candidates are haphazardly made by the split function at the split node. Among those, the candidate that amplifies the data increase about the relating node is chosen. The data gain ΔE is effectively determined by entropy estimation given by the equation.

$$\Delta E = \frac{|Il|}{|In|} E(I_l) - \frac{|Ir|}{|In|} E(l_r) \quad (9)$$

There are two conditions that can conclude the iterative training. The primary condition happens in case there is no more data increase conceivable. The subsequent condition happens, if the preparing procedure arrives at a leaf node that is at the greatest depth of the tree. Thus a leaf node has a posterior likelihood and the class disseminations P (c/n) and assessed experimentally as a histogram of class c_i of the preparing models that arrived at node n. The test picture is utilized as input to the prepared random forest. The ultimate class distribution is produced by gathering of each dispersion of all trees $L = (l1, l2, l3, , , , , , lr)$ by utilizing the following equation.

$$P(c_i/L) = 1/T \sum_{t=1}^{T} P(c_i/lt) \quad (10)$$

Where T is the number of trees and we select c_i as the last class of an input picture if $P(c_i/L)$has the most extreme values.

4.2 Multi- Layer BPNN (Back Propagation Neural Network)

BPNN (Back Propagation Neural Network) is a method for preparing multi-layer ANN (Artificial Neural Network) [13]. It is a multi-layer forward system utilizing to expand gradient descent based delta learning rule known as back propagation. It gives a computationally efficient strategy for changing the loads in a feed forward system with differentiable function work units to get familiar with a training set of input yield being a gradient descent strategy; it minimizes the full squared error of the yield computed by the system. The system is prepared by supervised learning strategy. The basic structure of the BPNN incorporates one input layer at least one hidden layer followed by the output layer. Neural system works by modifying the weight values during preparing, so as to lessen the error between the real and desired output design [14]. The goal of this system is to prepare the network to achieve an adjustment between the capacity to react accurately to the input designs that are utilized for training and the ability to give great reaction to the input that are similar.

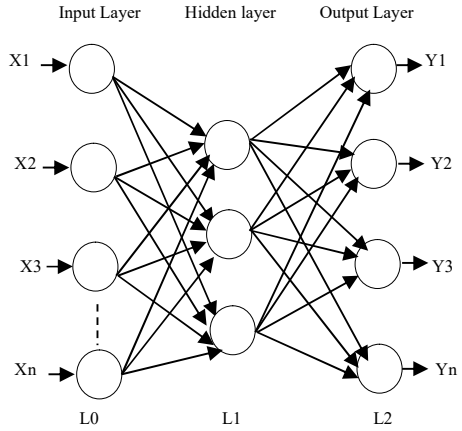

Figure 6 Back Propagation Neural Network

It has three kinds of layers Input layer, Hidden layer and output layer. Hidden layer does middle computation before guiding the input to output layer. Moreover back propagation can be considered as a generalization of delta rule. At that point when the back propagation system is cycled an input pattern is proliferated forward to the output units through the interceding input to hidden layer and then hidden to output weights. It consists of numerous layers of computational units, normally interconnected in a feed forward manner. Each neuron in one layer has coordinated associations with the neurons of the subsequent layer. In numerous applications, the units of these systems apply a sigmoid function as an enactment work function. All inclusive estimation hypothesis for neural system states, that each continuous function, that maps interims of genuine numbers to a few output interims of genuine numbers can be approximated discretionarily intently by a multi-layer preceptor with only one hidden layer.

This outcome holds just for confined class of activation functions. Multi-layer system [15] utilizes an assortment of learning methods, the most well-known back propagation. In this the output values are compared with the proper reply to compute the estimation of a few predefined error functions. By different systems, the error is then encouraged back through the system. Utilizing this data, the algorithm adjust the weight of each association in arrange so as to decrease the value of the error function just barely. After repeating this procedure for an adequately expansive number of preparing cycles, the system will more often than not to meet to a few states, where the error of the calculation is little.

4.3 Adaboost SVM

Adaboost with SVM based component classifier is generally considered to break the Boosting rule for the trouble in preparing of SVM and have lop-sidedness between the difference and exactness over fundamental SVM classifiers. The Adaboost classifier within the paper trains SVM as base classifier with changing kernel function parameter σ value, which continuously diminishes the changes of weight value in training test. To affirm the legitimacy of the classifier, the classifier is tried on human subjects to classify the right and left knee effusion imagery tasks. The running time for preparing algorithms for SVM can be diminished, if just a barely any preparing illustrations are included with the real calculations. This truth can be exploited by Adaboost, if at every cycle most of the weight within the distribution passed to the powerless learner is allocated to many information points. The calculation time can be diminished as pursues. One of the off chances if the complexity of the original preparing calculations is bounded by $A\mathrm{m}^{x}$ with $A \in R$ at that point training with a fraction vm is

bounded by $A(vm)^x$. Hence, preparing q speculations is bounded by $Aq(vm)^x$. Then if$x > 1{,}0 > v > 1$, and $q \leq 1/v$.

$$Aq(vm)^x < \frac{A}{v}(vm)^x = Av^{x-1}m^x \leq Am^x \quad (11)$$

The classification execution of Adaboost SVM is affected by its parameters. For SVM-RBF, the parameters are Gaussian width σ and regularization parameter C. SVM-RBF classifiers performance generally depends on the σ value in case a generally appropriate C is choosen [22]. For a given C, the performance of SVM-RBF can be changed by essentially altering the value of σ. Expanding the value often decreases the complexity of learner model and bringing down the classification execution and vice-versa. So when the SVM-RBF is utilized as powerless classifier for Adaboost, a moderately huge value is liked, which brings a SVM-RBF with moderately powerless learn capacity [23].

The Adaboost calculation makes a set of destitute learners by keeping up a collection of weights over training information and alters then after each powerless learning cycle adaptively. The weights of the training samples which are misclassified by current frail learner will be expanded while the loads of the tests which are accurately grouped will be diminished. One of the fundamental thought of Adaboost algorithm is to keep up a circulation over the preparing set. The weight of this dispersion on preparing model i on round t is signified $D_t(i)$. At first, all loads are instated similarly, however on each round; the loads of erroneously classified cases are increased, so that the frail learner is forced to center on the difficult illustrations within the exchanging set. The feeble learner responsibility is to discover a frail theory $h_t: x\{-1, +1\}$ suitable for the appropriation $(D)_t$. Given: (x_1, y_1),…… ,(x_n, y_n) where $x_1 \in X$, $y_1 \in Y = \{-1, +1\}$.

When applying Boosting strategy to solid component classifier, these component classifiers must be suitable depilated in arrange to advantage from boosting. Consequently, if SVM-RBF is utilized as component classifier in Adaboost, a generally expansive value, which corresponds to a SVM-RBF with generally powerless learning ability, is favoured. In the proposed Adaboost SVM, without loss of simplification, the re-weighting strategy is used to refresh the loads of preparing tests. Adaboost can be depicted as pursues.

At first, a huge worth is set to σ, comparing to a SVM-RBF classifier with exceptionally feeble learning capacity. At that point, SVM-RBF with this σ is prepared, however many cycles as conceivable under the circumstances as long as beyond more than half exactness can be gotten. Otherwise this σ worth is diminished marginally to expand the learning capacity of SVM-RBF to enable it to accomplish the more than half accuracy. By diminishing the σ value marginally, this avoids the new SVM-RBF from being solid for the current weighted preparing tests, and hence decently exact SVM-RBF segment classifiers are acquired. The reason why moderately exact SVM-RBF component classifiers are favoured lies in the way that these classifiers regularly have bigger assorted variety than those segment classifiers which are exceptionally exact. These bigger assorted varities may prompt a superior speculations execution of Adaboost. This procedure proceeds until the σ is diminished to the given insignificant value.

5 Experiments and Results

This experimental study was taken on 203 patients. MRI images have been collected from different medical institutes. Most of the image size was 350 x 350 pixels and some of the image size was 630 x 630 pixels. To maintain the uniformity, the image is resized into 250x250 pixels. From the obtained pictures, some of the already available pictures are in grayscale mode and the remaining of the

pictures which was not accessible in the grayscale has been changed over to the grayscale picture. In the pre-processing mode weiner filter is utilized to remove the noise from the image. To separate the region of interest, watershed segmentation is utilized. Utilizing the Gradient Magnitude as the segmentation function, first it divides the frontal area objects. Picture gradients have been utilized to extract data from a picture. Every pixel of the inclination picture estimates the adjustment in intensity from a similar point in the first picture in a specific heading. To obtain the address range, the gradient picture is determined in the x and y directions.

With the assistance of Watershed Transform Segmentation function, undesirable background data, for example content and other data had been expelled from the knee joint MRI picture; Watershed Transform is also utilized in this issue. The Watershed Transform identifies “catchment bowls” and “Watershed limits” in the picture by regarding it as a surface where light pixels are high and dim pixels are low. Segmentation that utilizes DAS transforms functions admirably in the event, so that we can recognize or “mark” objects in the foreground and background areas. Binary Marker controlled watershed segmentation pursues this basic procedure:

1 Calculate the dim area; it encourages us to distinguish the segmentation regions. Apply the Binary mask.

2 To compute the foreground, interconnect the blobs of pixels inside every one of the objects.

3 Background markers will considered the pixels that are not part of any object.

4 Expel the foundation blobs

5 Calculate the Watershed Transform of the altered Segmentation function

Subsequently after extracting the desired region, Gabor features are extracted from the picture. Gabor filters have been utilized in numerous applications, for example texture segmentation, objective detection, fractal measurement, report investigation, detection of an edge, picture coding and picture representation [24]. Initial step of Gabor feature extraction is to create a custom sized Gabor filter bank. It makes a u by v cell array, whose components are m by n matrices, each matrices being a 2-D Gabor filter. The next step is to extract the Gabor features from an input picture. It makes a column vector compromising of the Gabor features of an input picture. The feature vectors are standardized to zero mean and unit change.

Classification is final step to produce the result. For classification, three classifiers have been utilized namely Random Forest, BPNN and Boosting SVM are tested independently. In Random Forest, in the root node we pick r = 2, an extremely small number, to reduce the correlation between the resulting trees. For each node, we utilized r = 100D, where D is the depth of the node. In classification trees, the splitting decision is depending on the following strategies:

- Gini Index - It's a measure of node purity. If the Gini index takes on a small value, it recommends that the node is pure. For a split to take happen, the Gini index for a child node ought to be not as much as that for the parent node.
- Entropy - Entropy is a proportion of node impurity. For a binary class (a, b), the formula to calculate it is shown below. Entropy is most extreme at p = 0.5. For p (X = a) = 0.5 or p(X = b) = 0.5 means, another perception has a half chance of getting classified in either classes. The entropy is least when the probability is 0 or 1.

$$\text{Entropy} = - p(a)*\log(p(a)) - p(b)*\log(p(b)) \quad (12)$$

When choosing a binary test randomness is injected into the training set per tree: one third of the training pictures per class are arbitrarily choosen and are used to determine the node tests by the entropy basis and the rest of the training pictures are utilized to estimate the posterior probabilities in the terminal nodes. This heuristic involves randomizing over both tests and training data. When utilizing the simpler approach, trees are developed by randomly selecting n and b without measuring the gain of each test, and all the training pictures are utilize to estimate the posterior probabilities.

The Classification procedure is done with Boosting SVM. Normally, AdaBoost classifiers are having less tuning parameters compared to SVM and SVM is not influenced by the noise affectability. This tuning parameter is fundamentally utilized for improving the performance of classifiers. Here, the kernel function is utilized to improve the performance of the SVM. This system gives the RBF kernel for mapping the information into high dimensional space. The RBF kernel function is a best measurement for finding the similarity between normal and abnormal images. This comparability will be computed by utilizing the texture feature and the corners of the shape feature.

Back-propagation is the core of neural network training. It is the technique for calibrating for the loads of a neural net dependent on the error acquired in the previous iteration. Appropriate tuning of the loads permits us to reduce the error rates and to make the model dependably by expanding its speculation. The randomly acquired starting synaptic load of the neural system covers a range between -0.5 and 0.5. Best strategy for testing a neural system is to test a software application, if all the inclusion conditions are fulfilled. It iteratively learns a lot of loads for expectation of class mark tuples. The anticipated out is contrasted with the target value to check the error. This algorithm is a kind of supervised learning and utilized in feed forward neural system to prepare the system. The output of these classifiers is carried out. Those outputs are given in Table1, Table 2 and table 3 respectively.

.

Table 1: Results obtained from Random Forest Classifier

TYPE	TPR	FPR	TNR	FNR
Normal	0.9818	0.6000	0.4000	0.0182
Abnormal	0.9685	0.4375	0.0315	0.9318

Table 2: Classification Metric for Random Forest

TYPE	Precision	Specificity	Sensitivity	Accuracy	Error Rate
Normal	0.9474	0.4000	0.9818	0.9333	0.0667
Abnormal	0.9318	0.4375	0.9685	0.9091	0.0909

Table 3: Results obtained from Adaboost with SVM

TYPE	TPR	FPR	TNR	FNR
Normal	0.9623	0.7143	0.2857	0.0377
Abnormal	0.9449	0.5000	0.5000	0.0551

Table 4: Classification Metric for Adaboost with SVM

TYPE	Precision	Specificity	Sensitivity	Accuracy	Error Rate

Normal	0.9107	0.2857	0.9623	0.8823	0.1167
Abnormal	0.9375	0.5000	0.9449	0.8951	0.1049

Table 5: Results obtained from Back Propagation Neural Network

TYPE	TPR	FPR	TNR	FNR
Normal	0.9636	0.6000	0.4000	0.0364
Abnormal	0.9603	0.5294	0.4706	0.0397

Table 6: Classification Metric for BPNN

TYPE	Precision	Specificity	Sensitivity	Accuracy	Error Rate
Normal	0.9464	0.4000	0.9636	0.9167	0.0833
Abnormal	0.9308	0.4706	0.9603	0.9021	0.0979

The average accuracy rate 88.92% is calculated from Adaboost with SVM, 90.94% is calculated from BPNN and 92.12% is calculated from Random Forest.

6 Discussion

We report the advancement and approval of a mechanized framework for quantitative volume assurance of knee joint effusion in MRI pictures. Two conventions intended to approve the created innovation, one utilizing adjusted phantoms and another going for examination with a manual strategy, indicated magnificent reproducible outcomes. Further, correlation between the joint effusion volume obtained by MRI pursued by evaluation with the created computerized framework and the immediate desire performed on knee OA patients additionally showed a superb connection.The MRI convention incorporated a T1-and a T2-weighted pivotal arrangement. The decision of axial arrangements came about from the need to lessen incomplete volume impact on the division of the joint effusion. In view of the fundamental direction of the synovial pocket along the bones, the other obtaining planes, sagittal and coronal, would have delivered progressively fractional volume. In spite of the fact that the T2 grouping improved the joint emission signal, the other liquid like tissues, for example, blood, a few hyaline cartilage, and bone marrow sores, too showed up brilliant. Subsequently, the utilization of intensity property just would not be adequate to segment the joint effusion dependably. In this way, the bone was utilized as an anatomic reference for 3D item filtering. T2 arrangement does not give a maximal differentiated signal for the bone, the T1 grouping was utilized for the division of the femur and tibia, as they show up more clear and progressively homogeneous on the picture.

Conclusion

The effusion of knee joint is a typical finding in OA patients and might be identified with the action of the disease. Accordingly non-invasive completely computerized evaluation of joint effusion volume in the knee would be an important apparatus for indicative, development and clinical investigation. The detailed automatic framework for joint effusion evaluation approved by outer methods, manual

MRI evaluation and direct goal was demonstrated to be exact and precise, in expansion to preventing intra and inter-observer varities. The responsiveness to alter of automatic assessment of joint effusion ought to be additionally tried in al longitudinal examination in perspective on its future application in clinical research. In spite of an assessment of clinical tests to evaluate joint effusion in knee OA, the larger part of unstandardized test had generally low intraand inter-observer unwavering quality. Unwavering quality and demonstrative accuracy seems to be made with involvement. Compared to indidual tests employing a combination of tests for effusion seem to improve affectability. There is inadequately proof to suggest a specific test in clinical practice. Clinical involvement and effusion profundity may influence the accuracy of clinical examination in identifying knee effusion in patients with knee osteoarthritis. MRI may help clinicians in accomplishing a more precise determination, superior therapeutic decision, as well as objective measure in clinical outcomes. In this work we have utilized two feature extraction processes namely Watershed segmentation and 2-D Gabor Filter were computed. For classification purpose, Random Forest, Multi-layer BPNN and Adaboost SVM are employed. When compared to the classification result one with each other, Random Forest gives the best accuracy than other two classifiers for this work. The proposed method has achieved the maximum classification accuracy rate of 92.12%. In conclusion the knee joint effusion was not static in more in older adults. It was prescient of, but not predicted by other structural variations from the normal, recommended a potential part in early knee OA changes.

References

1. *Ekman L, Nilsson G, Persson L, Lumsden JH: Volume of the synovia in certain joint cavities in the horse. Acta Vet Scand **1981**, 22:23-31.*
2. *Hong BY, Lee JI, Kim HW, Cho YR, Lim SH, et al. (**2011**) Detectable threshold of knee effusion by ultrasonography in osteoarthritis patient. Am J Phys Med Rehabil 90: 112- 118.*
3. *Orthopaedics One Articles, orthopaedic knowledge network.*
4. *Johnson MW (**2000**) acute knee effusions: a systematic approach to diagnosis. Am Fam Physician 61: 2391-2400.*
5. *Blewis ME, Nugent-Derfus GE, Schmidt TA, Schumacher BL, Sah RL (**200**7) A model of synovial fluid lubricant composition in normal and injured joints. Eur Cell Mater 13: 26-39.*
6. *Sturgill LP, Snyder-Mackler L, Manal TJ, Axe MJ (**2009**) Interrater Reliability of a Clinical Scale to assess Knee Joint Effusion. J Orthop Sports Phys Ther 39: 845-849.*
7. *Kraus VB, Stabler TV, Kong SY, Varju G, McDaniel G: Measurement of synovial fluid volume using urea. Osteoarthritis Cartilage **200**7, 15:1217-1220.*
8. *J. Kamarainen, V. Kyrki, and H. Kalviainen, "Invariance properties of Gabor filter-based features-overview and applications," IEEE Trans. Image Processing, vol. 15, no. 5, pp. 1088–1099, **2006**.*
9. *K. He, J. Sun, and X. Tang, "Guided image filtering," in European Conf. on Computer Vision, **2010**, pp. 1–14.*
10. *S. Qiu, F. Zhou, and P. E. Crandall, "Discrete Gabor transforms with complexity O (nlogn)," Signal Processing, vol. 77, no. 2, pp. 159–170, **1999**.*
11. *O. Nestares, R. F. Navarro, J. Portilla, and A. Tabernero, "Efficient spatial-domain implementation of a Multiscale image representation based on Gabor functions," J. Electronic Imaging, vol. 7, no. 1, pp. 166–173, **1998**.*
12. *P. Yin, A. Criminisi, J. Winn, and I. Essa. Tree-based Classifiers for Bilayer Video Segmentation. In Proc. CVPR, **2007**.*
13. *Shylaja S & et.al. "Feed Forward Neural Network Based Eye Localization and Recognition Using Hough Transform", International Journal of Advance Computer Science and Applications, Vol.2, No.3, pp.104-108, March **2011**.*
14. *Daugman. J, "High Confidence visual Recognition of Persons by a Test of Statistical Independence", IEEE transactions on Pattern Analysis and Machine Intelligence, Vol. 15, No. 11, pp. 1148-1161, **1993**.*

15. *C. Ben Abdelkader, R. Culter, H. Nanda, and L. Davis, "Eigen Gait: Motion-Based Recognition of People Using Image Self-Similarity," Proc. Int'l Conf. Audio- and Video-Based Biometric Person Authentication, pp. 284-294,* ***2001***.
16. *Soille, P.: Morphological Image Analysis - Principles and Applications. In Springer-Verlag Berlin Heidelberg (****1999****) 316.*
17. *Nassir Salman, "Image Segmentation Based on Watershed and Edge Detection Techniques'' The International Arab Journal of Information Technology, Vol. 3, No. 2, April* ***2006.***
18. *Jos B.T.M. Roerdink and Arnold Meijster, "The Watershed Transform: Definitions, Algorithms and Parallelization Strategies'' Fundamental Informaticae 41 (****2001****) 187–228.*
19. *S. BEUCHER, "The Watershed Transformation Applied To Image Segmentation", Centre de Morphologie Mathématique Ecole des Mines de Paris 35, rue Saint-Honoré 77305 Fontainebleau Cedex (France).*
20. *Md. Shakowat Zaman Sarker, Tan Wooi Haw and Rajasvaran Logeswaran, Morphological based technique for image segmentation, International Journal of Information Technology, Vol. 14, No. 1.*
21. *A. Bieniek, A. Moga, An efficient watershed algorithm based on connected components, Pattern Recognition 33, pp.907-916,* ***2000***.
22. *G.Valentini, T.Dietterrich. Bias-variance analysis of support vector machines for the development of Svm-based ensemble methods. Journal of Machine Learning Research.* ***2004****(5):725-775.*
23. *X.Li, L.Wang, E.Sung. A Study of AdaBoost with SVM Based Weak Learners. Proceedings of International Conference on Neural Networks,* ***2005****:196-200.*
24. *T. P. Weldon, W. E. Higgins, and D. F. Dunn, ``Gabor filter design for multiple texture segmentation,'' Optical Engineering, vol. 35, no. 10, pp. 2852-2863, Oct.* ***1996***.